

Ising spin glass that closely resembles the physical glass transition

Marc L. Mansfield

Department of Chemistry and Chemical Biology, Stevens Institute of Technology, Hoboken, New Jersey 07030

(Received 17 September 2001; published 2 July 2002)

We consider a modification of the one-dimensional Ising model in an external field in which the higher-energy spin state is assumed to be P -fold degenerate. The model shows a transition that becomes first order in the limit of infinite coupling constant. Here we report a study of the dynamical properties of the model by computer simulation in the vicinity of this transition, under the assumption that the model evolves by single spin flips with Metropolis bias, but with certain forbidden flips. The result is a model that exhibits many well-known empirical properties of the physical glass transition, including the “Kauzmann paradox,” the Vogel law, stretched-exponential relaxation, and dynamic heterogeneity.

DOI: 10.1103/PhysRevE.66.016101

PACS number(s): 05.50.+q

I. INTRODUCTION

Empirical evidence for spatially heterogeneous dynamics in supercooled liquids is now available from a number of laboratories. The glass transition seems to be related to the coexistence of two types of small domains with fast and slow dynamics, respectively. The domains themselves appear to be dynamic, shifting their structure over time [1–4]. There is also modeling evidence that these domains are stringlike [5,6]. Mean-field treatments, such as the mode-coupling model [7], are unable to provide a complete description of this heterogeneity. I present here a one-dimensional Ising model that is simple enough that results can be obtained without resorting to mean-field approximations. But it also displays many empirical properties of physical glasses, including the “Kauzmann paradox,” the Vogel law, stretched-exponential relaxation, and the dynamic heterogeneity mentioned above. It is formally equivalent to the one-dimensional Ising model in an external field, which, of course, means that its equilibrium properties can be treated rigorously, while its dynamical properties can be simulated with considerable ease. The model also displays a first-order phase transition in one limit, although the interesting glassy properties are not observed in this limit. Other authors have discussed glassy Potts models, but typically in mean-field approximation [8], and have also suggested that “random first order” transitions underlie the physical glass transition [9].

Formally, we will assume that there are $P+1$ spin states, which might be labeled $0, 1_1, 1_2, \dots, 1_P$. However, the P states $1_1, 1_2, \dots, 1_P$ are assumed to be completely degenerate, and we define a composite state, 1, so that effectively the model has only two states, 0 and 1. A spin in state 1 has equal probability of being in any of the states $1_1, 1_2, \dots, 1_P$. $\sigma_j = 0$ or 1 represents the spin state of spin j . Spins in states 0 and 1 contribute energies of 0 and 1, respectively. Each nearest-neighbor pair of spins contributes energy 0 when in the same state, and m when in different states. We refer to sequences of 1-spins as clusters, and sequences of 0-spins as gaps, with the chain consisting of alternating clusters and gaps. The coupling constant m is therefore the boundary energy between clusters and gaps. For reasons to become obvious in Sec. III, we exclude from the ensemble the chain all

of whose spins are 0. Therefore, all states of the system contain at least one cluster.

Since 1-spins have higher energy and degeneracy than 0-spins, there exists a temperature, $T_0 = 1/\ln P$, such that the system prefers either 0- or 1-spins depending on the value of T relative to T_0 . Ordinarily, and especially in one dimension, we do not expect to see strong nonlinearities in the vicinity of T_0 . However, by assigning a large value to m , we are able to introduce a bias towards long-range order since the total number of boundaries will diminish if like spins group together. Indeed, when m is large, strong nonlinearities at temperatures near T_0 are observed.

II. EQUILIBRIUM PROPERTIES

The following transfer matrix controls the equilibrium properties of this model:

$$\mathbf{T} = \begin{bmatrix} 1 & Pxy \\ y & Px \end{bmatrix}, \quad (1)$$

where

$$x = \exp(-1/T), \quad y = \exp(-m/T) \quad (2)$$

and where T represents temperature. The eigenvalues of \mathbf{T} are

$$r_{\pm} = 2^{-1} \{ 1 + Px \pm [(1 - Px)^2 + 4Pxy^2]^{1/2} \}. \quad (3)$$

The partition function is given rigorously by

$$Z = \text{tr}(\mathbf{T}^N) - 1 = r_+^N + r_-^N - 1. \quad (4)$$

The subtraction of unity removes the contribution of the chain of all 0's. Since $r_+ > r_-$ always, and $r_+ > 1$ at all $T > 0$, the approximation $Z = r_+^N$ is valid at all temperatures except within $O(1/\ln N)$ of absolute zero. Specifically, it is only at such extremely low temperatures that the neglect of the all-0 chain becomes significant. Table I displays a number of equilibrium properties.

Note that as $y \rightarrow 0$, $r_+ \rightarrow \max(1, Px)$ while $r_- \rightarrow \min(1, Px)$. Therefore, in the small y limit, we observe a slope discontinuity in the free energy as a function of tem-

TABLE I. Equilibrium properties of the model. The following properties can all be derived from the transfer matrix. \mathbf{T}' is the matrix whose second column equals the second column of \mathbf{T} , but whose first column contains zeros.

Property	Value in thermodynamic limit
The partition function Z	r_+^N
Free energy per spin A	$-T \ln r_+$
Probability that an arbitrary spin is in state 1 P_1	$(x/r_+) (\partial r_+ / \partial x)$
Cluster density P_c	$(y/2r_+) (\partial r_+ / \partial y)$
Total energy per spin E	$P_1 + 2mP_c$
Spatial spin correlations $\langle \sigma(0)\sigma(j) \rangle$	$Z^{-1} \text{tr}[(\mathbf{T}', \mathbf{T}^{j-1}, \mathbf{T}', \mathbf{T}^{N-j-1})]$
Correlation function: $S(j) = \{ \langle \sigma(0)\sigma(j) \rangle - \langle \sigma \rangle^2 \} / \{ \langle \sigma^2 \rangle - \langle \sigma \rangle^2 \}$	$(r_- / r_+)^{j-1}$, neglecting front factor
Spatial correlation length Γ	$[\ln r_+ - \ln r_-]^{-1}$
Average gap length G	$(1 - P_1) / P_c$
Average cluster length C	P_1 / P_c
Gap length distribution (unnormalized) g_j	$(1/r_+)^j, j=0,1,2,\dots$
Cluster length distribution (unnormalized) c_j	$(Px/r_+)^j, j=0,1,2,\dots$

perature and the system displays a first-order phase transition at the temperature $T_0 = (\ln P)^{-1}$. There is, of course, a well-known proscription against first-order phase transitions in one-dimensional systems, but since this system only displays the transition in the limit $y \rightarrow 0$, there is no violation of the theorem. Nevertheless, when y is near but distinct from 0, the transition is abrupt but not discontinuous. Figures 1–3 display the temperature dependence of the populations of 1-spins and clusters, of the energy and entropy, and of the heat capacity, $\partial E / \partial T$, calculated with $m=5$ and $P=2$, for which $T_0 \approx 1.44$.

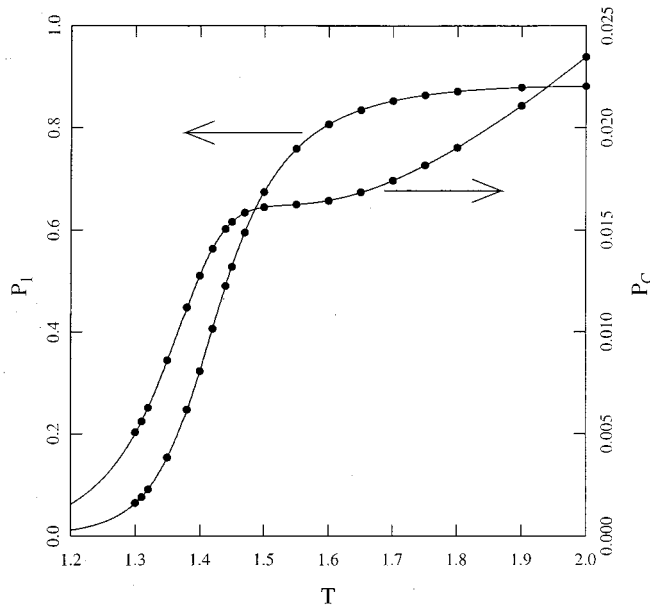


FIG. 1. Densities of 1-spins (P_1) and of clusters (P_c). The scale for P_c is expanded 40-fold relative to that for P_1 . Symbols are simulation results; curves are calculated according to formulas in Table I. In this and all subsequent figures, energy units are such that the energy difference between 0- and 1-spins is 1 and temperature units are such that Boltzmann's constant is 1.

We recover the standard Ising model by setting $P=1$, which shifts the transition temperature to $T_0 = \infty$. However, in the limit of infinite temperature, y as defined approaches 1, and the transition would not be observed. Therefore, to see the transition when $P=1$, we would need to make the coupling constant proportional to T . Then it would occur at the zero of reciprocal temperature, at the switch from large positive to large negative temperatures.

The spatial correlations $\langle \sigma(0)\sigma(j) \rangle$ are the probabilities that spins 0 and j are simultaneously in state 1. The difference $\langle \sigma(0)\sigma(j) \rangle - \langle \sigma \rangle^2$ proves to be proportional to $(r_- / r_+)^j = \exp(-j/\Gamma)$, for the correlation length Γ defined as

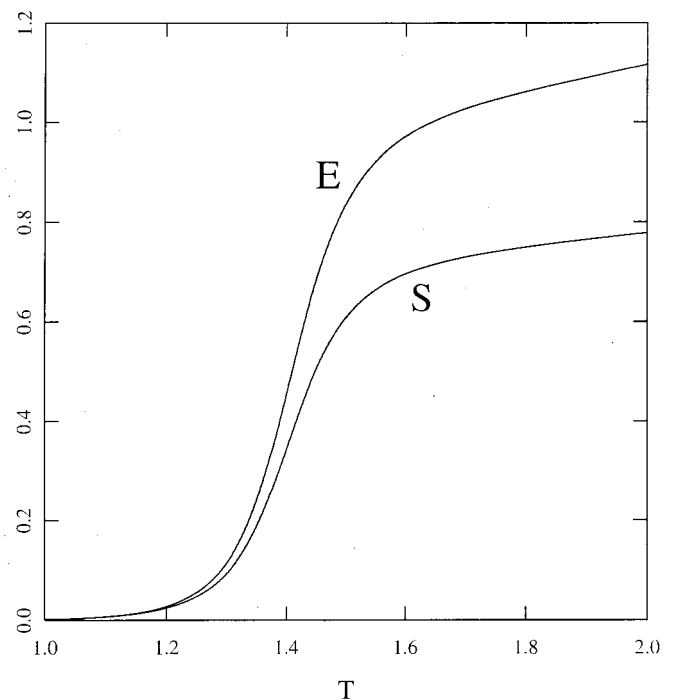


FIG. 2. Energy and entropy per spin as functions of temperature.

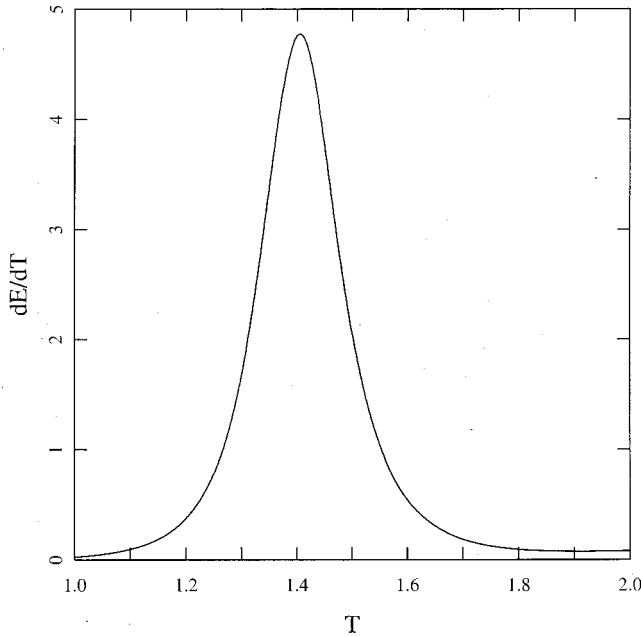


FIG. 3. Heat capacity per spin as a function of temperature.

in Table I. Near T_0 , Γ is $\approx 1/(2y)$, so that with strong coupling, correlations become long-ranged. This heterogeneity is, in part, responsible for glassy behavior, as we shall see.

The average lengths of gaps and clusters are shown in Fig. 4. Gaps and clusters dominate, respectively, at low and high temperatures. Also, as observed in Table I, clusters and gaps have Poisson length distributions.

III. DYNAMICAL PROPERTIES

We consider the dynamics of the model in discrete time with Metropolis sampling. The fundamental dynamical process is single-spin flipping, but certain transitions, $\dots 000 \dots \leftrightarrow \dots 010 \dots$ and $\dots 100 \dots \leftrightarrow \dots 110 \dots$ are forbidden. The first constraint prevents the spontaneous appearance or disappearance of an isolated 1-spin; in other words, a cluster of length one. The second constraint prevents movement of the right boundary of a cluster. Table II summarizes the dynamical process. Although the right boundary of any given cluster is pinned, the left boundary moves via the process $\dots 001 \dots \leftrightarrow \dots 011 \dots$. Furthermore, clusters are created and destroyed by the division or the union of existing clusters via the process $\dots 101 \dots \leftrightarrow \dots 111 \dots$.

Obviously, any possible arrangement of clusters and gaps can be generated from any other arrangement: We permit the left boundary of all clusters to move through repetitions of the process $\dots 001 \dots \rightarrow \dots 011 \dots$ until all gaps have length 1, then fill these gaps through the process $\dots 101 \dots \rightarrow \dots 111 \dots$. We can then work in reverse to generate any new configuration. The only inaccessible state is the chain of all 0's. So to rigorously satisfy ergodicity, we exclude this state from the ensemble. As mentioned above, in the thermodynamic limit this omission is only significant in a vanishingly small interval near absolute zero.

As a result of the process $\dots 001 \dots \leftrightarrow \dots 011 \dots$, the left edge

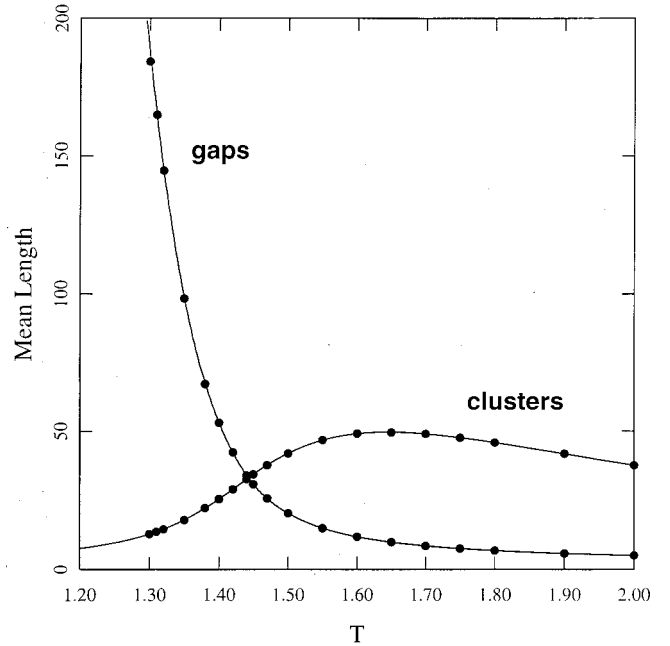


FIG. 4. Mean lengths of clusters and gaps. Symbols are simulation results; curves are calculated according to formulas in Table I. Lengths are measured relative to the lattice spacing of the model.

of any given cluster performs a biased random walk, with steps to the left and right occurring with relative weights Px and 1, respectively. At temperatures $T > T_0$, the bias is toward the left ($Px > 1$), the gaps are narrow and tend to shrink spontaneously so that the clusters have relatively short lifetimes; and we need not wait long to see any given cluster quenched by a cluster to its right. At temperatures $T < T_0$, the bias is towards the right ($Px < 1$), the gaps have a broad Poisson length distribution, and any given cluster can have a very long lifetime as we wait for the cluster at its right to grow and quench it. Cluster lifetimes are distributed broadly and increase on average with falling temperature. This ex-

TABLE II. The model evolves dynamically via single spin flips with Metropolis bias, but with certain forbidden flips. A single spin σ_j is selected at random. The second column gives the probability with which σ_j flips and is a function of the spin states of the two neighboring spins. The system clock then advances by the amount $1/N$, for N the total number of spins. Here $Q = (P+1)^{-1}$. (These transition probabilities are only valid when $m > 0.5$.)

Initial configuration $\dots \sigma_{j-1} \sigma_j \sigma_{j+1} \dots$	Transition probability
$\dots 0 0 0 \dots$	0
$\dots 0 1 0 \dots$	0
$\dots 1 0 0 \dots$	0
$\dots 1 1 0 \dots$	0
$\dots 0 0 1 \dots$	QP_x
$\dots 0 1 1 \dots$	Q
$\dots 1 0 1 \dots$	QP
$\dots 1 1 1 \dots$	Qy^2/x

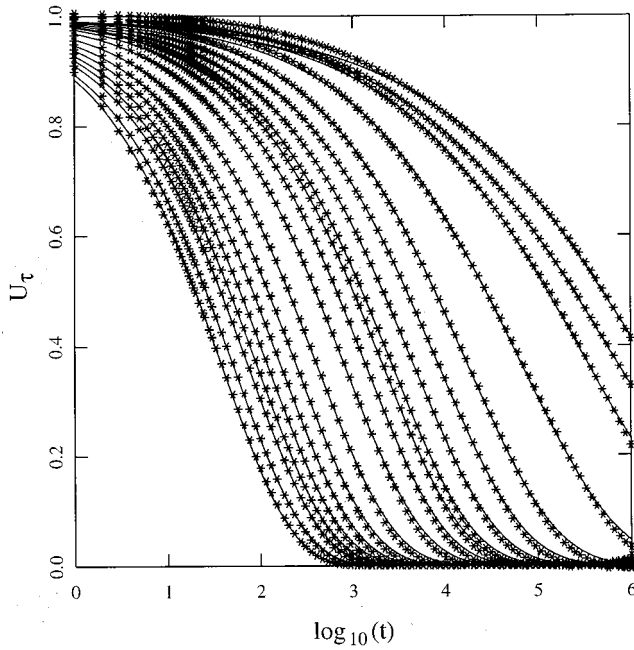


FIG. 5. Simulation data for the time correlation function $U_\tau(t)$ over a range of temperatures between $T=1.3$ and $T=2$. Symbols are the simulation data; solid curves are the best-fit stretched-exponential functions. Time units in this and subsequent figures are such that N attempted spin-flips represent one unit of time.

plains the glassy behavior of the system.

We define variables τ_j such that $\tau_j=1$ if and only if $\sigma_j=1$ and $\sigma_{j+1}=0$; in all other cases $\tau_j=0$. The τ_j 's label the right edges of all the clusters, and are convenient dynamical markers for the clusters: The period of time over which a spin has τ state of 1 is precisely the life-span of the associated cluster.

We consider two correlation functions:

$$U_\tau(t) = \frac{\langle \tau_j(0)\tau_j(t) \rangle - \langle \tau_j \rangle^2}{\langle \tau_j^2 \rangle - \langle \tau_j \rangle^2}, \quad (5)$$

$$U_\sigma(t) = \frac{\langle \sigma_j(0)\sigma_j(t) \rangle - \langle \sigma_j \rangle^2}{\langle \sigma_j^2 \rangle - \langle \sigma_j \rangle^2}, \quad (6)$$

where $\tau_j(0)$, $\tau_j(t)$, $\sigma_j(0)$, and $\sigma_j(t)$ are the values of τ_j and σ_j at times 0 and t , respectively. We have estimated these correlation functions by computer simulation. A number of trajectories, each of length 10^6 time steps, were generated at a series of temperatures, using the values $P=2$, $m=5$, and $N=1000$. With $P=2$, we have $T_0 \approx 1.44$. For simple spin systems such as these, an initial random configuration can be obtained easily from the transfer matrix using Meirovich's scanning technique [10], which is rigorous as long as the full system is scanned. Therefore, annealing to achieve equilibrium is not necessary. $U_\sigma(t)$ and $U_\tau(t)$ were calculated by direct sampling along each trajectory at a series of t values with approximately uniform logarithmic spacing and at a series of different temperatures. The values obtained at each temperature were then fitted to the stretched-exponential relaxation function

$$\exp[-(t/t_R)^\beta] \quad (7)$$

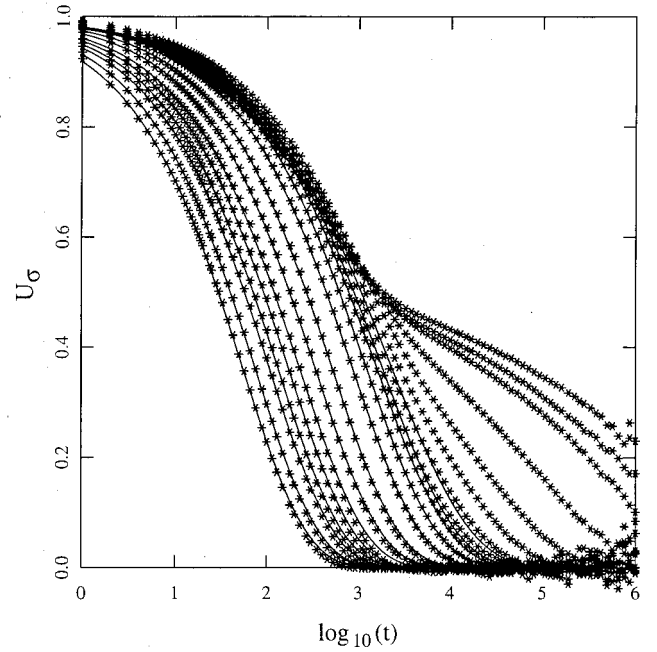


FIG. 6. Simulation data for the time correlation function $U_\sigma(t)$ over a range of temperatures between $T=1.3$ and $T=2$. Symbols are the simulation data; solid curves are the best-fit stretched-exponential functions.

by linear regression of $\ln[-\ln U_x(t)]$ vs $\ln t$ (but using only those values for which $0.1 < U_x(t) < 0.9$). Figures 5 and 6 display the two relaxation functions at a series of temperatures. The stretched-exponential function provides a good fit for both U_τ and U_σ at high temperatures, but only of U_τ at all temperatures. U_τ probes the lifetime of individual clusters, its relaxation time, $t_{R\tau}$, can be construed as the cluster lifetime. U_σ , on the other hand, probes the flipping motion of individual spins, and at low temperatures two separate relaxations become resolvable. The faster relaxation arises from the fluctuating motion of individual clusters as they grow and shrink, while the slower relaxation arises from the creation and annihilation of clusters. This faster relaxation is suggestive of the α relaxation in real liquids. Interestingly, the separation into two time scales appears at the temperature T_0 . Further study of the U_σ function is obviously needed, while for now we examine only U_τ . Figures 7 and 8 display the temperature dependence of the stretched-exponential parameters $t_{R\tau}$ and β_τ characterizing U_τ . The parameter $t_{R\tau}$, representing the cluster lifetime, varies with temperature according to the empirical Vogel law,

$$t_{R\tau} = A \exp[B/(T - T_V)] \quad (8)$$

with $A=4.63$, $B=1.74$, and $T_V=1.165$. The stretched-exponential index β_τ decreases slowly with decreasing T at temperatures $T > T_0$, and much more rapidly as we pass below $T=T_0$. The relaxations of many physical phenomena are well represented by the stretched-exponential function, with relaxation times following the Vogel law. Furthermore β is usually observed to decrease with decreasing temperature. In fact, examples are known in which the rate of decrease of

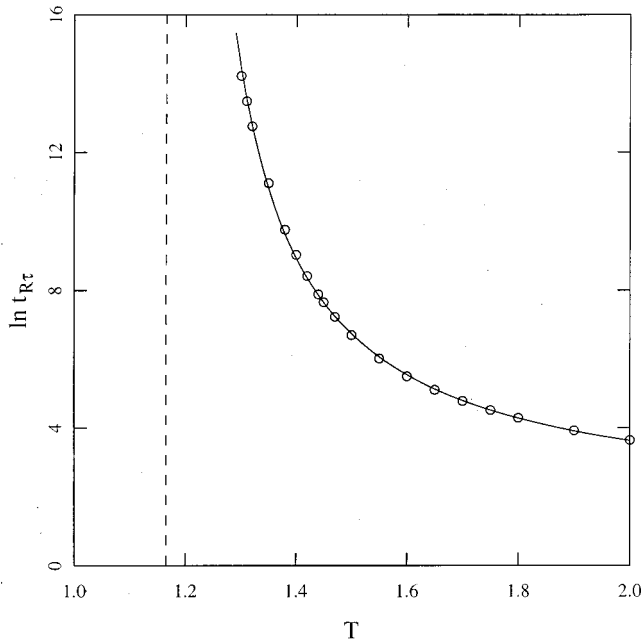


FIG. 7. Relaxation time $t_{R\tau}$ as a function of temperature. Symbols are the simulation data; solid curve displays the best-fit Vogel function. The vertical dashed line gives the value of the Vogel temperature.

β changes dramatically in qualitative agreement with Fig. 8 [11]. We note that the glass transition temperature, defined as the point at which the Vogel law appears to diverge, is $T_V \approx 1.16$, substantially lower than the transition temperature $T_0 \approx 1.44$.

At $T = 1.3$, the relaxation time exceeds 10^6 , and this temperature proves to be the practical limit of simulation. As many trajectories as needed were run to bring the sampling error in U_τ and U_σ within acceptable bounds, but this requires many more trajectories at lower temperatures. (At $T = 1.3$, about 1000 independent trajectories were needed; about 400 at each of the temperatures 1.31 and 1.32; 100–300 when $1.35 \leq T \leq 1.44$; and 20–50 when $1.44 < T$.)

IV. DISCUSSION AND CONCLUSIONS

This model reproduces all of the following empirical properties of glass-forming liquids: (1) The energy and entropy fall off rapidly upon cooling (see Fig. 2), in agreement with the behavior often referred to as the Kauzmann paradox. (2) The temperature dependence of the relaxation time follows the Vogel law. (3) The spectrum of relaxation times broadens upon cooling in agreement with the stretched-exponential law. (4) Spatially heterogeneous dynamics, i.e., coexisting domains of, respectively, fast and slow relaxation, present at equilibrium and which constantly move about, are observed. A fifth property, two separate time scales at low temperatures, displayed in the U_σ correlation function and suggestive of the empirical α relaxation, can also be cited, but further study of the temperature dependence of these two time scales is needed.

It might be argued that the empirical heat capacities do

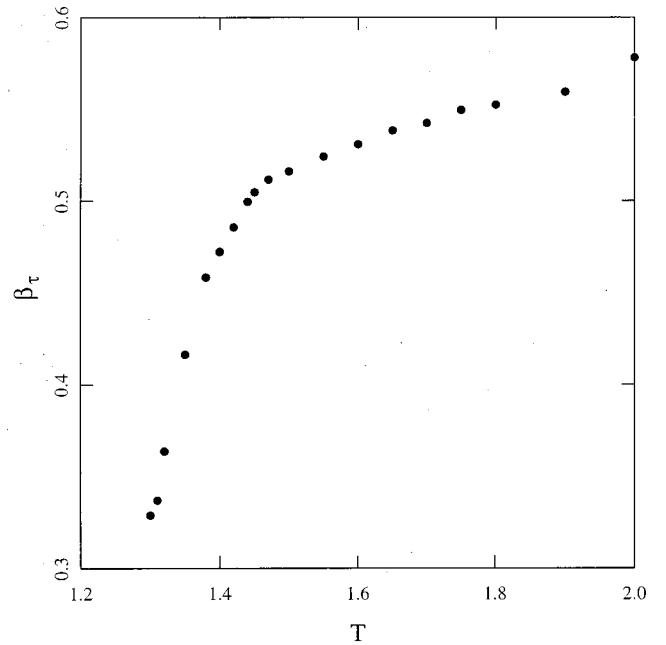


FIG. 8. Stretched-exponential index β_τ as a function of temperature.

not exhibit the strong peaks displayed in Fig. 3. However, it should be remembered that the glass transition is a configurational effect. This model is construed only to represent the configurational contribution to the heat capacity. We can expect any such peaks in real systems to be significantly washed out by vibrational contributions. Furthermore, the fact that the system eventually leaves equilibrium upon cooling means that the measured heat capacity will not exhibit a peak as strong as that shown in Fig. 3.

Let us summarize the features of the model that lead to glassy behavior. First, a relatively large coupling constant promotes inhomogeneity. Second, because the clusters have higher spin entropies than the gaps ($\ln P$ vs 0), the temperature $T_0 = 1/\ln P$ marks a transition from cluster dominance to gap dominance. The combination of these two effects produces highly nonlinear behavior near T_0 . And third, the two dynamical constraints, suppression of spontaneous cluster creation and annihilation and the pinning of clusters by not permitting their right boundaries to move, produce glassy dynamics, since cluster quenching can only occur when two clusters merge. The process of cluster formation and destruction spreads out over a broad range of times because the gap distribution is broad.

One question concerns the generalization of this model to higher dimensions, since higher-dimensional Ising models display richer phase behavior. However, the relevant transition occurs at infinite temperature in the standard model, and would seemingly be unaffected by, for example, the Ising critical point. We are currently studying the behavior of this model in higher dimensions.

Assuming that some generalization of this model can be applied in higher dimensions, we can then ask what the model teaches us about supercooled liquids. The model sug-

gests several assumptions about real liquids, which we discuss in the following.

(1) *Supercooled liquids possess two separate “phases.”* This model suggests that supercooled liquids exhibit two separate equilibrium “phases”; an “ideal” liquid and an “ideal” glass phase, analogous, respectively, to the clusters and gaps of the model. We enclose the term “phases” in quotes because they are not true macroscopic phases; clusters and gaps have a finite average size and at macroscopic length scales the system is uniform. In liquids, the two phases apparently are structurally similar, both being disordered packings, although the ideal glass is less energetic and less degenerate than the liquid. The clusters represent regions of high internal mobility, since each 1-spin is actually in one of P different degenerate states.

(2) *Liquid domains at their minimum size have relatively low entropy but high energy.* The smallest cluster is a single 1-spin, and has entropy $\ln P > 0$ and energy $2m \gg 1$. The model therefore suggests that in real liquids, for whatever reason, the smallest liquid domains have high energies and low entropies, in the sense that their energies and entropies are much larger than and comparable to, respectively, that which would be expected based solely on the bulk energy and entropy, respectively, of the phase.

(3) *Ideal liquid and ideal glass domains may grow and shrink at the expense of one another, but liquid domains cannot spontaneously disappear; they must be quenched by another domain.* The dynamics of the model has been constrained to forbid a cluster from spontaneously disappearing. In order to quench a liquid domain, another domain must grow and coalesce with it. At low temperatures, this is a rare occurrence, since the equilibrium concentration of domains is small. This also produces a broad spectrum of quenching times for liquid domains, since the gaps between domains obey a Poisson distribution. Therefore, this assumption is

what gives rise both to the stretched-exponential relaxation and to the Vogel temperature dependence.

It is obviously too early to insist that this model represents the actual behavior of real liquids. It may be that the model captures all the essential phase space properties of true liquids without insisting that real liquids satisfy the three conditions listed above. A better understanding of the effect of dimensionality, as previously mentioned, will probably bear on this question. In any case, additional work is needed to understand exactly the relationship between this model and actual liquids.

For many supercooled liquids, the temperatures T_V [in Eq. (8)] and T_K (the temperature at which the extrapolated entropy, Fig. 2, appears to vanish) are nearly the same. For the model presented here, they are, respectively, 1.16 and about 1.3. Neither the reasons for nor the significance of this difference is understood at present.

Another area of study is the effect of the degeneracy term P on the model. In this work we have only studied the dynamics of the model given $P=2$. As suggested by a referee, changes in P might change the fragility of the system.

Additional work is also needed to understand the relationship between this model and other models of glassy behavior, most notably, mode-coupling theory [7]. One feature of mode-coupling theory is the “crossover temperature,” T_c , considerably above the empirical glass transition temperature, which marks a transition from normal liquid to glassy behavior. The temperature T_0 plays a very similar role in the current model.

ACKNOWLEDGMENT

The author acknowledges a number of helpful discussions with Dr. Jack F. Douglas of the National Institute of Standards and Technology.

-
- [1] M. D. Ediger, *Annu. Rev. Phys. Chem.* **51**, 99 (2000).
 - [2] M. D. Ediger and J. L. Skinner, *Science* **292**, 233 (2001).
 - [3] L. A. Deschenes and D. A. Vanden Bout, *Science* **292**, 255 (2001).
 - [4] E. V. Russell and N. E. Israeloff, *Nature (London)* **408**, 695 (2000).
 - [5] C. Donati, J. F. Douglas, W. Kob, S. J. Plimpton, P. H. Poole, and S. C. Glotzer, *Phys. Rev. Lett.* **80**, 2338 (1998).
 - [6] P. Allegrini, J. F. Douglas, and S. C. Glotzer, *Phys. Rev. E* **60**, 5714 (1999).
 - [7] W. Götze and L. Sjögren, *Rep. Prog. Phys.* **55**, 241 (1992).
 - [8] E. Marinari, S. Mossa, and G. Parisi, *Phys. Rev. B* **59**, 8401 (1999).
 - [9] X. Xia and P. G. Wolynes, *Proc. Natl. Acad. Sci. U.S.A.* **97**, 2990 (2000).
 - [10] H. Meirovitch, *J. Chem. Phys.* **89**, 2514 (1988).
 - [11] J.-W. Park, M. D. Ediger, and M. M. Green, *J. Am. Chem. Soc.* **123**, 49 (2001).